International Journal of Engineering Research & Technology (IJERT)
ISSN: 2278-0181
Vol. 4 Issue 09, September-2015

Preparation and Characterization of Different Tio_2-Modified Montmorillonite Meso-Microporous Materials, with Enhanced Photocatalytic Activity

Manel Baizig* (1), Soumaya Khalfallah(1), Bassem Jamoussi(2), Narjès Batis(1) and Raquel Trujillano(3)
[1] Unité de recherche de Catalyse d'Electrochimie de Nanomatériaux et leurs Applications et de Didactique (CENAD), Institut National des Sciences Appliquées et de Technologie (INSAT), Université de Carthage, Centre Urbain Nord B.P. n° 676-1080 Tunis Cedex –Tunisie
[2] Institut Supérieur d'Education et de Formation Continue (ISEFC) 43, rue de la Liberté 2019 Le Bardo-Tunisie
[3] Departamento de Química Inorgánica, Universidad de Salamanca, 37008 Salamanca, Spain

***Abstract*—A set of TiO_2-modified montmorillonite meso-microporous materials, as photocatalysts, was successfully prepared in different ways and evaluated by the photodegradation of 4-nitrophenol (4-NP) in water, since it is a recalcitrant organic pollutant.**

The effects of photocatalysts' preparation methods on their textural, structural and catalytic properties were tested. To understand the relationship between the photocatalysts structure and performance, these were characterized by X-Ray Diffraction (XRD), UV-spectroscopy, Scanning Electron Microscopy/Energy Dispersive X-ray spectroscopy (SEM/EDX), Fourier Transform Infrared Spectroscopy (FTIR), X-ray fluorescence (XRF), specific surface area and porosity measurements.

A high specific surface area (up to 231 m^2/g), a meso-microporous structure and a high stability have been found for the $TiCl_4$-M and $TiCl_3$-M prepared photocatalysts.

In addition, to improve the 4-NP degradation, various parameters' effect was studied such as the type of the photocatalyst, its amount loading, the pH of the 4-NP solution and the initial 4-NP concentration. Then, the 4-NP degradation rate has reached 99% only when Anatase Titanium dioxide was supported on montmorillonite, at pH=5, with 0.2 g/100 mL of photocatalyst ($TiCl_4$-M or $TiCl_3$-M) amount and a 4-NP concentration equal to 20 $mg.L^{-1}$.

***Key words*—Anatase Titanium dioxide; TiO_2-modified montmorillonite; meso-microporous materials; 4-Nitrophenol photodegradation improvement.**

I. INTRODUCTION

Montmorillonite clays, being classified as porous materials [1], are frequently studied and used as adsorbents and catalysts [2-4]. This is partly due to their exceptional properties such as high cation exchange capacity, good swelling, high surface area and high porosity [1-5]. These properties allow their modification for specific applications. In fact, they are generally used as support of other active species such as inorganic metal oxide particles [6]. Many studies have been reported the utilization of montmorillonite as support of Titania [2, 7, 8]. In fact, Anatase Titanium dioxide is the most known and attractive material, having a high photocatalytic activity and it is characterized by a large specific surface [9-11] [12]. It is frequently used in photocatalysis for wastewater treatment of many hazardous organic contaminants such as organic dyes [8], phenol compounds [13], pesticides [14] and herbicides [15].

However, when Titania is used in slurry form, it presents several practical disadvantages, like particle agglomeration [16] and the recovery of the powder after chemical reaction [12, 17-19] which needs a microfiltration (energetically costly and time consuming).

The use of clay as support seems to be a good solution to solve these problems. There are different kinds of clays that have been used as a support such as bentonite [20], zeolite [21], kaolinite [22], sepiolite [23], and montmorillonite [24].

In this study, we have chosen a montmorillonite clay as support for titania for its properties (low cost, no toxicity, high surface area and its swelling ability [25-27]).

Therefore a series of TiO_2-supported montmorillonite porous materials has been prepared employing various ways. The effects of titanium source and the preparation methods on the structural, textural and photocatalytic properties of these materials have been investigated. TiO_2-modified montmorillonite was prepared firstly by hydrolysis of $TiCl_4$ according to the method presented by Sterte [28]. Secondly, it was made using a solution of $TiCl_3$, as an intercalation solution, based on the method presented by Jianjun Liu et al. [19]. Thirdly, an interaction solution of Titanium isopropoxide is used following the method described by Yamanaka et al [29].

The performance of different prepared photocatalysts was tested for the photodegradation of 4-nitrophenol in presence of UV-irradiation. The degradation rate was improved by the determination of optimal operating parameters and by the study of the effects of various experimental parameters, essentially the photocatalyst type, its amount loading, the initial concentration and the pH of 4-nitrophenol solution. To understand the relationship

between the photocatalysts structure and performance, different methods of characterization (X-ray diffraction, UV-spectroscopy, infrared spectroscopy, EDX/MEB, BET specific surface area, X-ray fluorescence) were used.

II. MATERIALS AND METHODS:

A. *Chemicals and reagents:*

Montmorillonite K10, titanium (IV) isopropoxide and titanium (IV) chloride (99.9%) were provided by sigma-aldrich.
Titanium (III) chloride solution 15% in hydrochloric acid was supplied by Riedel de Haën.
4-nitrophenol (99%) was purchased from Merck.

B. *Photocatalysts preparation:*

1) The starting Na-montmorillonite:

The starting Na-montmorillonite was prepared after exchanging the commercial montmorillonite K10 with NaCl solution (1 $mol.L^{-1}$) and washing the clay several times with distilled water until it becomes free of Cl^- ions (proved by the test with $AgNO_3$). Washed clay was centrifuged, dried at 60°C and reffered as Na-mont.

2) Titanium-modified montmorillonite by hydrolysis of $TiCl_4$ ($TiCl_4$-M):

$TiCl_4$-M was prepared according to the protocol proposed by Sterte [28], with slight modification by hydrolysis of $TiCl_4$ with HCl. Preparation protocol is detailed in fig.1.

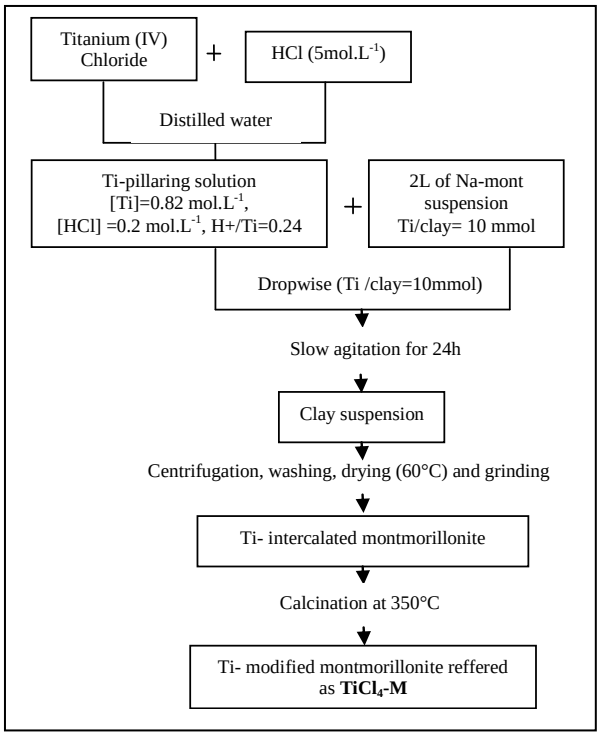

Fig.1 preparation protocol of $TiCl_4$-M

3) Titanium-modified montmorillonite by hydrolysis of $TiCl_3$($TiCl_3$-M):

According to the method presented by Jianjun Liu et al. [19], a solvothermal preparation was used to synthesize $TiCl_3$-M, using water and ethanol as solvent, hexamethylene tetramine as precipitant and titanium trichloride as precursor. More details are given in fig.2.

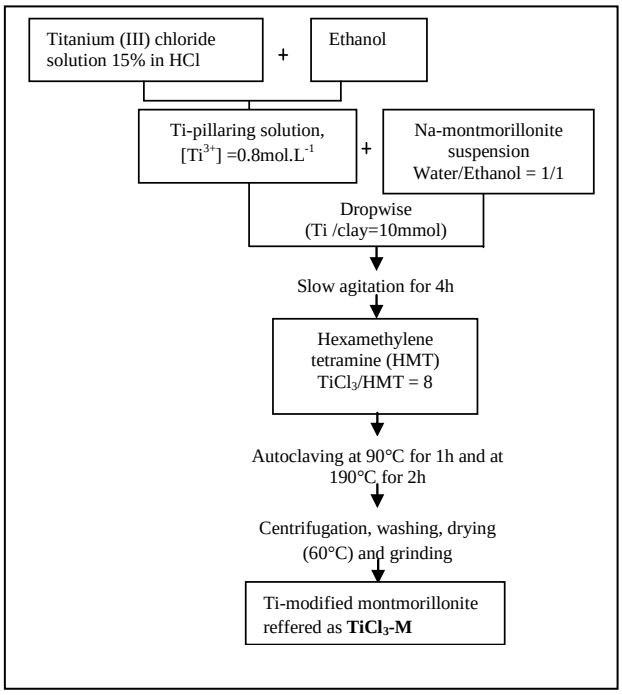

Fig.2 preparation protocol of $TiCl_3$-M

4) Titanium-modified montmorillonite by hydrolysis of $Ti(OC_3H_7)_4$(Iso-M):

Iso-M was obtained by the intercalation from $Ti(OC_3H_7)_4$, hydrolyzed with HCl as described by Yamanaka et al. [29] with slight modifications. Fig.3 illustrates the used protocol.

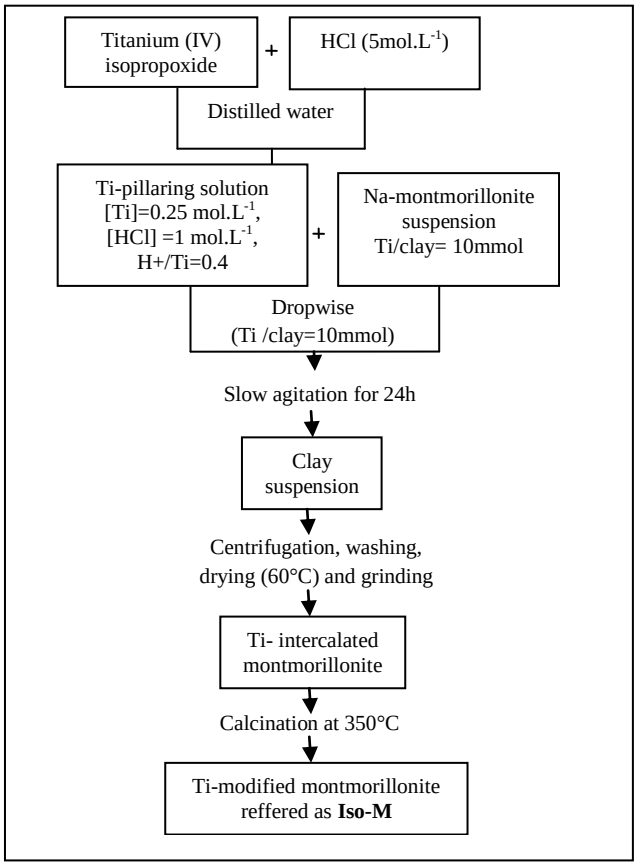

Fig.3 preparation protocol of Iso-M

C. Techniques of characterizations:

The powder X-Ray Diffraction (XRD) patterns were recorded with CuKα radiation (λ=1.5404Å) on a Siemens D-500 diffractometer (2°/min). The diffractograms were treated by "Diffract-AT" Software.

The specific surface areas, pore volumes and micropore volumes of the samples were measured by nitrogen physisorption at 77 K using a Gemini VII apparatus from micromeritics, the different photocatalysts were treated under vacuum for two hours at 110°C to evacuate water and gas pore.

The Fourier-Transform Infra Red (FTIR) spectra of prepared photocatalysts were carried out by KBr pellets technique using a Perkin Elmer FT 1730 instrument.

The UV-Vis spectra were recorded in a range of 190 to 800 nm using a HP 8453 Diode Array Spectrophotometer.

Analyses by Scanning Electron Microscopy with Energy Dispersive X-ray spectroscopy (SEM/EDX) images were taken at Servicio de Microscopía Electrónica (Universidad de Salamanca) on Zeiss microscopy from OXFORD Instruments.

The Chemical composition of the samples was determined by X-Ray Fluorescence (XRF) using a Magix PW2403 instrument.

D. Photocatalytic Activity:

The photocatalytic activities of the prepared samples were evaluated by the degradation of 4-nitrophenol aqueous solution under UV light irradiation.

The photocatalyst powder was dispersed in a 100 mL of 4-nitrophenol solution and kept under stirring, on a glass beaker equipped with a cooling system as shown in the fig.4. The experiments were conducted at different initial concentrations of 4-NP, at different photocatalyst amounts loading and by varying the pH of the initial solution. The pH of the solution was adjusted by tampon solutions. The suspension was air-oxygen-bubbled and irradiated with UV-light lamp (λ=253.7nm) which was emerged in the solution. Before irradiation, the suspension was stirred during 30 minutes in order to disperse the photocatalysts and to reach adsorption-desorption equilibrium between the organic molecule and photocatalyst surface.

During the reaction, every 10 minutes, a 2 mL of suspension solution was collected and filtered via syringe filter (0.45 µm). Then, the sampling was analyzed by UV-Vis Spectrophotometer Shimadzu 1650PC and by a standard High-Performance Liquid Chromatography apparatus Younglin Acme 9000 (Column type: Eclipse (C-18) (5 µm, 4.6 × 250 mm), at 20 µL injection, mobile phase: acetonitrile:water (40:60), and a fixed wavelength equal to 317 nm).

The degradation rate was deduced from the formula given by the following equation:

Degradation rate (%) = $(A_0-A_t/A_0)*100$

A_0: HPLC peak area of 4-NP initial solution.

A_t: HPLC peak area of 4-NP after a period of UV-light irradiation of suspension solution.

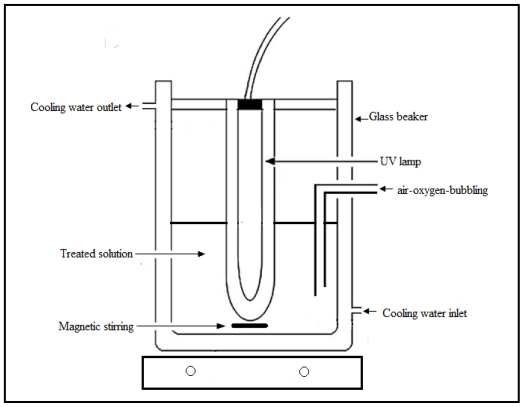

Fig.4 Descriptive schema of the photocatalytic reactor

III. RESULTS AND DISCUSSION:

A. photocatalysts characterization:

1) X-ray analysis:

Fig.5 shows X-ray powder diffraction patterns of the Na-mont, $TiCl_3$-M, $TiCl_4$-M, and Iso-M photocatalysts. The XRD pattern of Na-mont reveals the presence of diffraction peaks corresponding to Illite impurity (JCPDS file: 00-026-0911) and Quartz impurity (JCPDS file: 00-005-0490) which are observed at 2θ= 8.6°, 27.55°, 30.9°, 45.5° and at 2θ=20.6°, 26.4°, 49.9°, 59.7° respectively. A diffraction peak also appears at 2θ~5° which is commonly

assigned to the (001) Na-Mont diffraction peak corresponding to its basal spacing (d_{001}=15Å) [30]. This peak is weak although it is supposed to show a maximum intensity. This can be explained by a partial disordered structure. Actually, the K10-montmorillonite used is a synthetic clay previously activated by the fabricant with a mineral acid [31] which causes probably the partial delamination of its ordered and periodic structure [32]. Besides, different peaks characteristic of montmorillonite (JCPDS file: 00-013-0135) are detected in this pattern, these are located at 2θ=17.55° (d_{003}=5.04Å), 19.6° (d_{100}=4.52Å), 29.6° (d_{005}=3.01Å), 34.75° (d_{110}=2.57Å), 36.3° (d_{006}=2.47Å), 42.2° (d_{007}=2.14Å) and 61.6° (d_{0010}=1.5Å).

In $TiCl_3$-M diffraction pattern, the (001) diffraction weak peak is shifted to a lower value of 2θ (4.7°). This displacement reveals the increase of the basal spacing to 18.78 Å after intercalation. This result indicates an expansion in the layer structure; it is a proof of a successful pillaring [33]. New diffraction peaks appear in this pattern compared to the Na-mont pattern, these are observed at 2θ=25.15°, 37.8°, 47.75°, 54.8° and 62.25°. Referred to JCPDS file 00-21-1272, these diffraction peaks can be assigned to anatase phase. Thus, this result illustrates that the employed process is efficient to immobilize TiO_2 onto the clay.

However, the XRD patterns of $TiCl_4$-M and Iso-M are characterized by the absence of (001) diffraction peak. This reveals the complete loss of periodic structure of montmorillonite, which can be probably caused by the damage of the clay layers by acid conditions of the intercalation process [34]. The characteristic diffraction peaks of anatase phase are identified in the $TiCl_4$-M pattern at 2θ=25.35°, 37.75° and 48.05° but they are absents in the Iso-M pattern except the weak peak at 25.35°. TiO_2 seems to be immobilized in the case of $TiCl_4$ -M but not considerably for Iso-M.

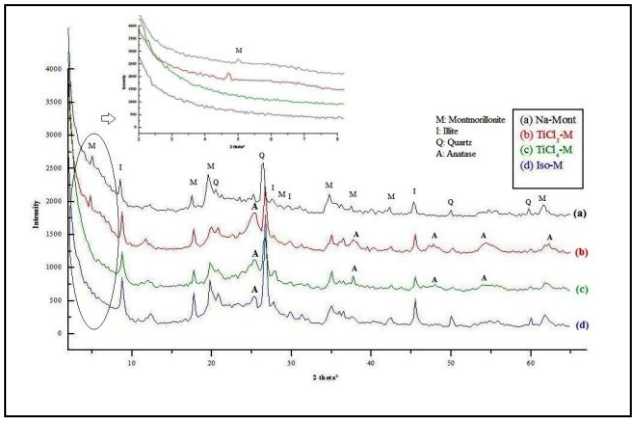

Fig.5 X-ray patterns of (a) Na-mont (b) $TiCl_3$-M (c) $TiCl_4$-M and (d) Iso-M.

2) FTIR analysis:

Fig.6 shows FTIR of the Na-mont spectrum, $TiCl_4$-M, $TiCl_3$-M and Iso-M. The principals bands detected in the spectra of Na-mont are summarized in the table 1.

TABLE.I FTIR BANDS OF NA-MONT

Band position	3624	3445	1639	1073	797	523	461
Intensity	medium and thin	Strong and broad	Medium and thin	Strong and broad	Medium and thin	Medium and thin	strong and thin

The absorption band centered at around 3445 cm^{-1} could be attributed to the stretching of the hydroxyl groups OH and to the vibration of physisorbed water between the clay layers [35].

The shoulder observed at about 3624 cm^{-1} is characteristic of montmorillonite [36].This shoulder corresponds to hydroxyl groups stretching vibration of the octahedral layer (Al and/or Mg…OH) [37-38]. Absorption band at around 1639 cm^{-1} is due to bending vibrations of water [37]. A large absorption band between 800 and 1200 cm^{-1} centered at 1100 cm^{-1} is generally observed for all silicates. In this spectrum, it is centered at 1061 cm^{-1} and corresponds to stretching vibration of Si-O [37-38].

Absorption band observed at around 797 cm^{-1} is relative to vibration of Hydroxyl groups coordinated to Aluminum (HO…Al) or octahedral Magnesium.

The absorption bands between 400 and 600 cm^{-1}, correspond to bending vibration of Si-O-Al^{VI}, Si-O-Mg^{VI} and Si-O-Fe liaisons of octahedral layer [37-38], in fact, two bands at 523 cm^{-1} and 461 cm^{-1} are located.

After the immobilization of TiO_2 on Na-mont, a disturbance of the bands located at 797, 523 and 461 cm^{-1} in the Na-mont spectra, is observed in the spectra of $TiCl_4$-M, $TiCl_3$-M and Iso-M. This disturbance is either explained by broadening of bands and/or by slight shift of their position and/or by overlap. This is probably due to the vibrations of Ti-O and Ti-O-Ti giving bands in the 400-800 cm-1 region [39-40]. In the spectrum of Iso-M, the band at 1073cm^{-1} broadens; this may be related to the fact of introduction of more –OH groups of the pillar after pillaring [41].

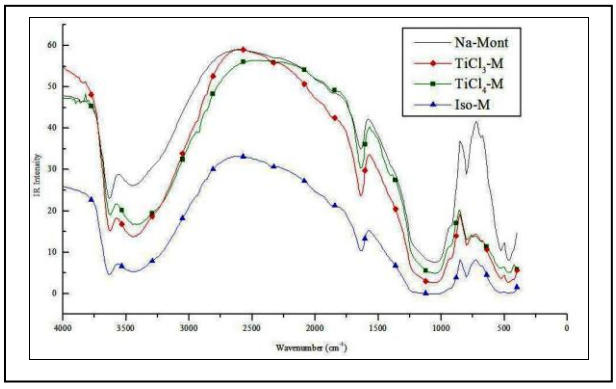

Fig.6 FTIR spectra of different samples

3) UV-Vis analysis:

The Na-mont UV-Vis spectrum (fig.7) shows that the sample is almost transparent beyond 350 nm, this is similar to the results reported by Oaka et al. [42]. In addition, a characteristic broad band centered at about 250

nm is detected, which is assigned to charge transfer band for the structural iron that is present in the octahedral layer of the clay mineral ($O^{2-} \rightarrow Fe^{3+}$; OH^- or OH_2) [43]. All the spectra of modified montmorillonites show that the samples don't absorb beyond 350 nm. But they present a new band centered at about 320 nm with different intensities. These new bands may be attributed to a charge transfer $O^{2-} \rightarrow T^{4+}$ of TiO_2 in anatase form [44]. The band intensity is probably proportional to the quantity of titanium dioxide fixed on the clay support.

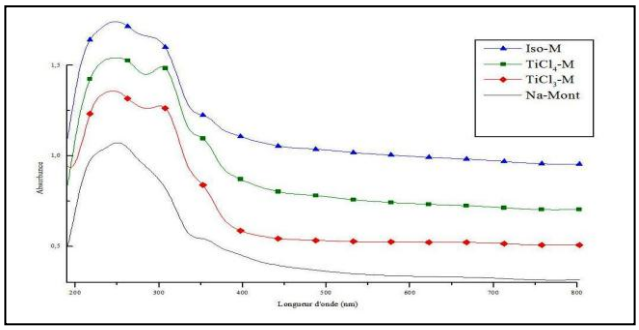

Fig.7 UV-Vis spectra of different samples

4) SEM and EDX analysis:

Fig.8 illustrates the morphology and elemental analysis composition of the modified montmorillonites which were explored using scanning electron microscopy with energy dispersive X-ray spectroscopy (SEM/EDX). Figure 8 (a-1) shows SEM micrograph of $TiCl_3$ displaying disordered distribution of aggregate particles with different shapes and sizes, there is an absence of ordered crystalline forms. Otherwise, multiple areas are in the forms of stratified layers or sheets which denote a partial ordered structure characteristic of clay materials [45-47].

Figures 8 (a-2) and 8 (a-3) represent respectively EDX micrograph and EDX spectrum of $TiCl_3$-M, taken on an area randomly chosen. EDX micrograph reveals the presence of titanium uniformly distributed throughout the montmorillonite. This is confirmed by the detection of titanium on the EDX spectra of the sample. Moreover, we denote the predominance of oxygen, silicon and aluminum with coexistence of few amounts of magnesium, calcium, potassium, iron, sodium and copper. These results indicate that even after modification the sample retains a characteristic chemical composition of the clay.

SEM images 8(b-1) and 8(c-1) of $TiCl_4$-M and Iso-M respectively present two irregular and disordered structures. The structure of the two modified clays appears to be strongly altered and disintegrated. $TiCl_4$-M particles are in "tatters" and between them we observe spheroid grains corresponding probably to TiO_2. These particles are

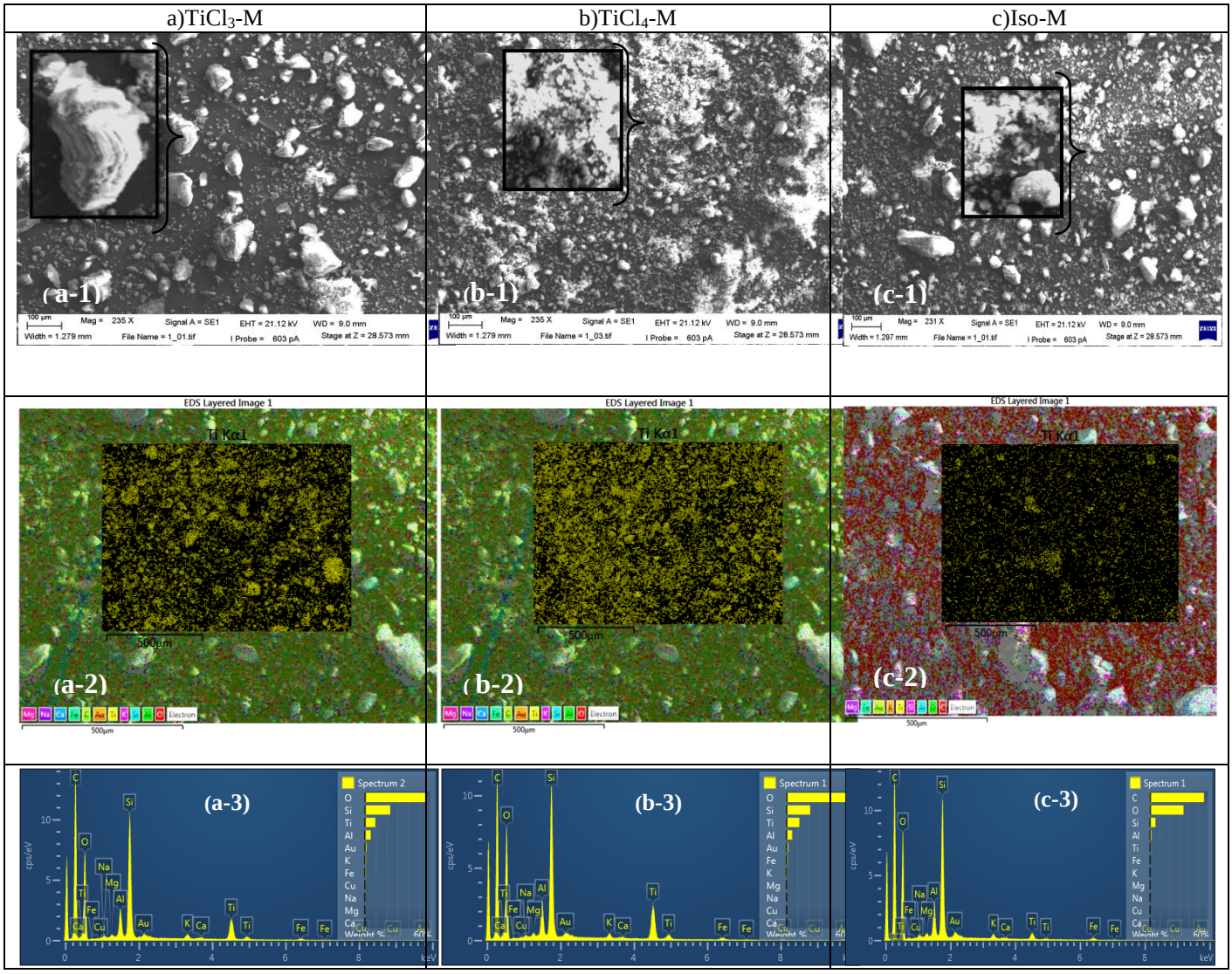

Fig.8 SEM micrographs and EDX micrographs and spectra of different samples

smaller and thinner than Iso-M particles which are in aggregate forms with different shapes and sizes.

We note the uniformity dispersion and the abundance of titanium in the $TiCl_4$-M micrograph shown in figure 8 (b-2). However the titanium is almost absent in the Iso-M micrograph presented in figure 8 (c-2). These results are also illustrated by the EDX spectra shown in figures 8 (b-3) and 8 (c-3). In fact, the $TiCl_4$-M spectrum reveals the presence of titanium unlike the Iso-M spectrum which titanium is detected in trace amounts. Results are similar to those found by DRX.

In accordance with the EDX spectrum of $TiCl_3$-M, the spectra of $TiCl_4$-M and Iso-M indicate the predominance of silicon, oxygen and aluminum and the presence in very low quantities of elements such as magnesium, iron, calcium, sodium, potassium and copper. So the basic structure of the montmorillonite is maintained after modification.

5) Textural analysis:

Fig.9 indicates the nitrogen adsorption- desorption isotherms of Na-Mont and TiO_2-modified montmorillonites. All isotherms can be considered as type II according to IUPAC classification, and they present hysteresis loops type H4 characteristic of materials with layered structure [48] and typical of slit-like pores [49]. Moreover, these isotherms shapes suggest the existence of both micropores and large pores in the samples. Actually, an increase in adsorbed volume at higher partial pressures was the result of larger mesopores presence [50].

TABLE II. RESULTS OF ADSORPTION- DESORPTION MEASUREMENT

Type of catalysts	m^2/g			cm^3/g		nm
	BET Surface Area	t-plot Micropore Area	t-plot External Surface Area	t-plot Micropore Volume	BJH Desorption pore volume	BJH Desorption pore Diameter
Na-mont	170	10.75	160.04	0.005	0.2616	5.12
$TiCl_3$-M	205	20.78	184.25	0.01	0.235	4.2
$TiCl_4$-M	231	0.9	230.48	0.002	0.205	3.65
Iso-M	183	18.26	165	0.01	0.238	4.98

Sodium montmorillonite has a specific surface area equal to 170 m^2/g (table.2), an average pore diameter equal to 5.12 nm typical of mesoporous materials; we also note the presence of micropores which occupy a surface of 10.75 m^2/g. This material is so specified by a bimodal porous distribution with mesopores dominance.

An increase of the specific surface area of $TiCl_3$-M is noted (table.2) compared to Na-Mont surface (from 170 m^2/g to 205 m^2/g) and a development of its microporous surface after insertion of TiO_2. This is possibly due to its insertion between the clay layers [19]. These results corroborate those obtained by DRX; in fact, we observed an increase in the basal spacing of clay from 15 Å to 18.78 Å which is probably caused by the formation of titanium dioxide pillars between the sheets [33]. These pillars generate space between adjacent layers [51]. The average pore diameter and the pore volume decreased after modification. This is due to the introduction of TiO_2 in the pores [52].

$TiCl_4$-M has the highest specific surface (231 m^2/g) and its pore average diameter is about 3.95 nm (table.2) which is typical of mesoporous materials. The decrease of pore average diameter indicates probably the incorporation of TiO_2 into the pores. Micropore surface decrease from 10.45 m^2/g to 0.9 m^2/g, consequently, we can conclude that TiO_2 insertion blocks the micropores, [52] which makes them inaccessible to nitrogen molecules N_2[51]. The increase of specific surface of $TiCl_4$-M is induced essentially by the increase of mesopores number, concluding that the sample is a unimodal pore size distribution.

A little increase of Iso-M specific surface and an insignificant decrease of the pore average diameter are noticed after modification as reported on the table 2. Micropores surface extends from 10.75 m^2/g to 18.26 m^2/g. Indeed, this sample is characterized by a bimodal pore distribution dominated by mesopores. Textural change is probably due to structure delamination as previously demonstrated by X-ray and SEM results; however, these results don't show the TiO_2 immobilization on the material and suggest probably its failure. Perhaps, it is due to the formation of Ti-polymeric species (Ti-polyoxycations) in the pillaring solution [53-54], which are voluminous and could not be inserted onto the pores of the clay.

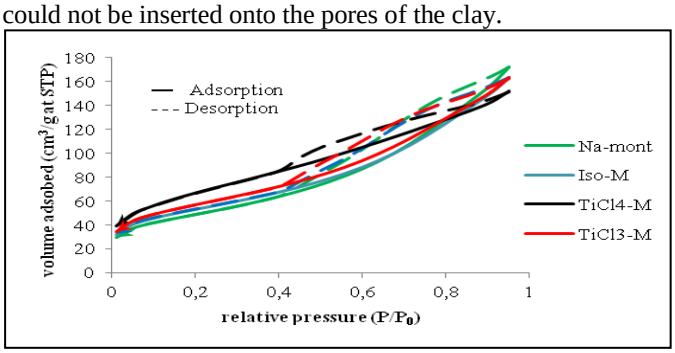

Fig.9 N_2 adsorption-desorption isotherms of different samples

6) Chemical analysis:

The results obtained previously were confirmed by chemical analysis shown in Table 3. Compared to Na-mont, a significant increase of TiO_2 content is observed in $TiCl_4$-M and $TiCl_3$-M, which indicates the immobilization of TiO_2, while the increase of TiO_2 content in Iso-M is slight. The increase of TiO_2 content in modified montmorillonites seems to be at the expense of Silicon, Aluminium and Iron contents.

TABLE III. CHEMICAL COMPOSITION OF NA-MONT AND TiO_2-MODIFIED MONTMORILLONITES

Oxyde %wt	SiO_2	Al_2O_3	Fe_2O_3	K_2O	MgO	P_2O5	**TiO_2**	SO_3	CaO	ZrO_2
Na-mont	71.68	16.18	5.07	2.72	1.50	1.18	**0.82**	0.25	0.18	0.06
$TiCl_3$-M	51.47	10.44	2.74	2.3	2.10	1.49	**28.9**	0.3	0.18	0.07
$TiCl_4$-M	51.09	11.47	3.84	1.91	2.10	0.88	**27.87**	0.26	0.17	0.07
Iso-M	65.3	14.3	4.29	2.58	2.6	0.88	**9.01**	0.42	0.22	0.06

B. photocatalytic activity improvement:

1) Effect of UV-light irradiation and photocatalyst addition:

100 mL of 4-NP solution (15 $mg.L^{-1}$) was prepared and 0.3g of $TiCl_4$-M (or $TiCl_3$-M) was added to evaluate the photocatalytic process of 4-NP degradation. Fig.10 shows the effect of the UV light irradiation and photocatalyst addition on the 4-NP degradation rate. In fact, we note that the 4-NP degradation did not occur in the presence of UV-light irradiation only. Adding the photocatalyst in the darkness, the 4-NP degradation rate did not exceed 11.46 %. This obtained rate is probably due to the adsorption of 4-NP into the clay [13]. The use of photocatalyst and the UV-light irradiation allows the 4-NP degradation at about 97% after 220 minutes. These results reveal that the 4-NP degradation can be achieved only in the presence of photocatalyst and UV-light irradiation and indicate that the decomposition of 4-NP is essentially caused by photocatalytic degradation but not adsorption [55].

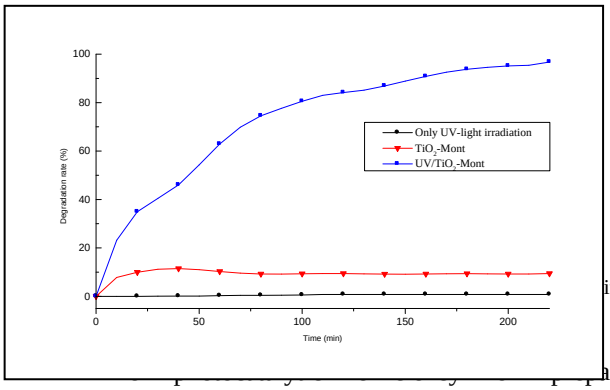

ition

ared

photocatalysts was tested by the degradation of a 4-NP solution (15 $mg.L^{-1}$) at 0.3g photocatalyst loading.

Fig.11 presents the effect of photocatalyst type on 4-NP degradation. In these curves we denote that Na-mont is relatively not photoactive and the low degradation rate obtained in this case and which did not exceed 8.6%, is caused probably by the adsorption of 4-NP onto the sample.

The degradation rate acquired over the Iso-M did not reach 40% after 220 minutes, which is low, this may be ascribed to its different structural and textural properties, actually, it present the lowest specific surface compared to other modified montmorillonite. In addition characteristic diffraction peaks of anatase phase were absent in its x-ray spectrum, also in its EDX spectrum titanium was detected in trace amounts.

Moreover, the $TiCl_4$-M and $TiCl_3$-M curves show that these two samples are efficient to degrade over 96% the 4-NP after 220 minutes. This is due to their interesting proprieties and morphologies. Their surfaces are porous and developed moreover characteristic diffraction peaks of anatase phase were detected in x-ray spectra and confirmed by the results obtained by SEM/EDX and chemical analysis.

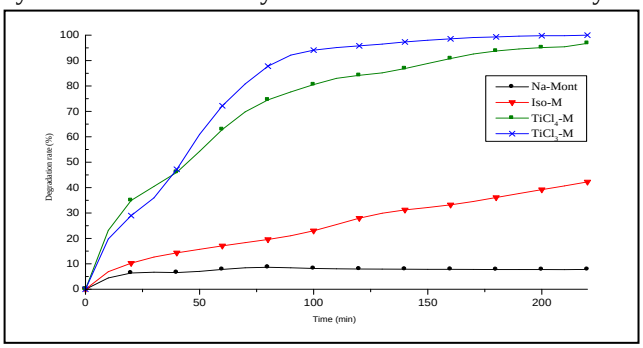

3) Effect of photocatalyst amount loading:

Photocatalyst loading is one of the major parameters which influence the degradation rate of organic compounds, that's why many investigations have been conducted in this regard [56-59].

In our study, we have followed, the influence of the photocatalyst amount increase added to a 4-NP solution (15 $mg.L^{-1}$), and UV-light irradiation during 120 minutes.

We found that the degradation rate is proportional to the photocatalyst loading until the value of 0.2 g/ 100 mL as shown in fig.12. These results can be explained by an increase of the active sites on the photocatalyst surface due to an increase in the photocatalyst amount, generating the hydroxyl radicals. However, when the photocatalyst amount exceeds the optimum value (0.2g/100 mL), it prevents the UV-light illumination, so the creation of HO· radicals' decreases and the efficiency of the degradation reduces [60-61].

Moreover, the excess of photocatalyst loading can induce the photocatalyst particles agglomeration which provokes the decrease of degradation rate [59].

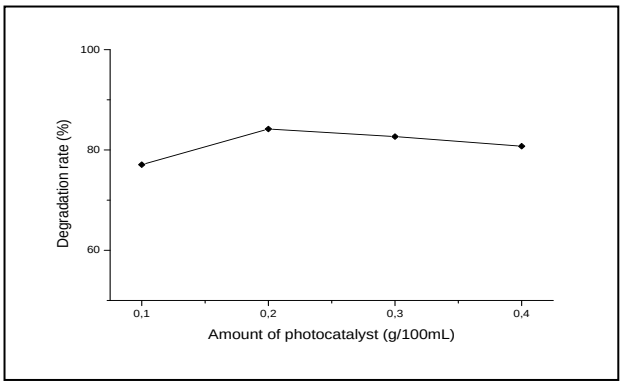

Fig.12 Effect of photocatalyst amount loading

4) Effect of the 4-NP solution pH:

The pH effect on the photocatalytic efficiency of organic pollutants has been studied by many researchers [62]. It was demonstrated that pH influences greatly the photocatalytic degradation of organic compounds. That's why we have investigated the effect of varying pH of 4-NP solution from 2 to 9 on the 4-NP degradation over $TiCl_4$-M (0.2 g/100mL) after 120 minutes light irradiation. As shown in fig.13, the increase of the pH from 2 to 5 raises the rate degradation from 46% to 84%. Beyond a value of pH=6, the rate degradation decreases.

A value of pH fixed to 5 should be chosen to achieve an ideal degradation rate. Therefore, the photocatalytic degradation is promoted in acidic medium since photocatalyst surface is positively charged while it is negatively charged in alkaline medium (pH>7). This can be explained by the ionization state of the surface corresponding to the following reactions [62]:

$TiOH + OH^- = TiO^- + H_2O$

$TiOH + H^+ = TiOH^{2+}$

In fact, in alkaline solution, a coulombic repulsion can be established between the negative charged surface of photocatalyst and the hydroxide anions which prevent the formation of $HO^{\cdot}$ and provoke the degradation decrease, whereas, the positive holes are the major oxidation species at low pH, that react with hydroxide ions to form hydroxyl radicals [62-64].

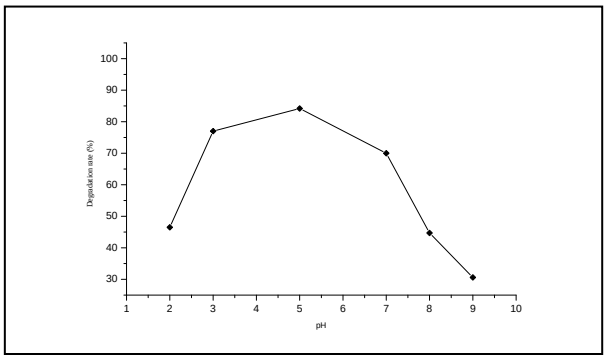

Fig.13 Effect of pH of the 4-NP solution pH

5) Effect of the 4-NP initial concentration:

Fig.14 shows the effect of the initial concentration of 4-NP on the 4-NP degradation over $TiCl_4$-Mont after 120 minutes, at pH 5 and 0.2 g/100 mL photocatalyst loading. Increasing the 4-NP concentration seems to decrease the 4-NP degradation rate. This can be explained by the fact of the increase of concentration which attenuates the UV-light that cannot pass through the solution and decreases the photocatalytic activity of the catalyst [55].

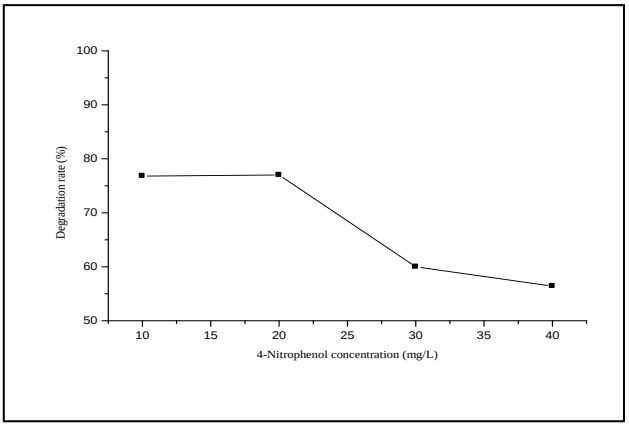

Fig.14 Effect of the 4-NP initial concentration

C. Conclusion:

The improvement of the photodegradation of the 4-NP has required the preparation of photocatalysts by immobilization of TiO_2 on montmorillonite nanocomposite by different methods.

The third method consisted to hydrolyze Titanium (IV) isopropoxide with HCl. Also, the acidic conditions employed in this process destroyed the ordered structure of the montmorillonite and allowed getting a delaminated meso-microporous structure. The immobilization of TiO_2 on the clay by this process did not took place efficiently because there was not a significant development of its specific surface area, the X-ray spectrum of this prepared sample did not reveal the presence of anatase phase and the EDX spectrum shows the presence of titanium in trace amounts. This photocatalyst was referred as Iso-M; the 4-NP degradation rate obtained did not exceed 40 %.

The first method was based on the reaction between Na-montmorillonite and acidic solution of hydrolyzed $TiCl_4$ with HCl. The resulting photocatalyst is named $TiCl_4$-M, it is characterized by a delaminated mesoporous structure. The acidic conditions of this process destroyed totally the periodic structure of the clay. But a developed specific surface area equal to 231 m^2/g was obtained, also characteristic peaks of anatase was detected on its x-ray spectrum and confirmed by the EDX and chemical analysis. This sample seems to be efficient to obtain a degradation rate over 96%.

The second method was a solvothermal preparation employing a $TiCl_3$-M as precursor, water and ethanol as solvent, and hexamethylene tetramine as precipitant. This method allowed obtaining a semi-ordered and meso-microporous structure, with a specific surface area equal to 205 m^2/g and with a basal spacing equivalent to 18.78 Å. It is characterized by the formation of anatase TiO_2. This sample was referred as $TiCl_3$-M, and by using it, a 4-NP degradation rate reached 99 %.

The study of the effect of various experimental parameters, essentially photocatalyst type, photocatalyst amount loading, 4-nitrophenol concentration, pH of 4-nitrophenol solution on 4-NP photocatalytic degradation, shows that to obtain an ideal degradation rate, the 4-NP degradation must be performed under UV-light irradiation, over 0.2g/100mL of $TiCl_3$-M or $TiCl_4$-M at pH=5.

ACKNOWLEDGEMENTS:

This work was financially supported by the Tunisian Ministry of High Education and Scientific Research. Authors thank the Departamento de Química Inorgánica de la Universidad de Salamanca (Spain) for its rich cooperation. N. Ben Messouad is gratefully acknowledged for her help in revising the English language of the paper and for XRF chemical analysis.

REFERENCES:

[1] A.K. Mishra, S. Allauddin, R. Narayan, T. M. Aminabhavi, K.V.S.N. Raju, "Characterization of surface-modified montmorillonite nanocomposites", Ceramics International 38 (2012) 929–934.

[2] R. Kun, K. Mogyorósi, I. Dékány, "Synthesis and structural and photocatalytic properties of TiO_2/montmorillonite nanocomposites", Applied Clay Science 32 (2006) 99–110.

[3] R. S. Varma, "Clay and Clay supported reagents in organic synthesis", Tetrahedron 58 (2002) 1235-1255.

[4] M.Baizig, B. Jamoussi, N. Batis, "Optimization by RSM of the degradation of three phenolic compounds – hydroquinone, resorcinol and catechol – on Fe-modified clays", Water Quality Research Journal of Canada 48.2 (2013) 171-179.

[5] Y. Xi, Z. Ding, H. He, R.L. Frost, "Structure of organoclays—an X-ray diffraction and thermogravimetric analysis study", J. Colloid Interface Sci. 277 (2004) 116–120.

[6] J.Praveen Kumar , P.V.R.K. Ramacharyulu, G.K. Prasad, Beer Singh, "Montmorillonites supported with metal oxide nanoparticles for decontamination of sulfur mustard", Applied Clay Science (2015).

[7] J. Ménesi, L. körösi, E. Bazso, V. Zöllmer, A. Richardt, I. Dékany, "Photocatalytic oxidation of organic pollutants on titania-clay composites", Chemosphere 70 (2008) 538-542.

[8] R. Djellabi, M.F. Ghorab, G. Cerrato, S. Morandi, S. Gatto, V. Oldani, A. Di Michele, C.L. Bianchi, "Photoactive TiO_2–montmorillonite composite for degradation of organic dyes in water", Journal of Photochemistry and Photobiology A: Chemistry 295 (2014) 57–63.

[9] M. Pelaez, A.A. de la Cruz, E. Stathatos, P. Falaras, D.D. Dionysiou, "Visible light activated N-F-codoped TiO_2 nanoparticles for the photocatalytic degradation of microcystin-LR in water", Catal. Today 144 (2009) 19–25.

[10] J.G. Yu, M.H. Zhou, B. Cheng, X.J. Zhao, "Preparation, characterization and photocatalytic activity of in situ N,S-codoped TiO_2 powders", J. Mol. Catal. A: Chem. 246 (2006) 176–184.

[11] Y.J. Chen, D.D. Dionysiou, "Bimodal mesoporous TiO_2–P25 composite thick films with high photocatalytic activity and improved structural integrity", Appl. Catal. B: Environ. 80 (2008) 147–155.

[12] D. Chen, Q. Zhu, F. Zhou, X. Deng, F. Li, "Synthesis and photocatalytic performances of the TiO_2 pillared montmorillonite", Journal of Hazardous Materials 235– 236 (2012) 186– 193.

[13] H. Ben Yahia Smida, B. Jamoussi, "Degradation of Nitroaromatic Pollutant by Titanium dioxide/Zinc Phthalocyanine: Study of the Influencing Factors", IOSR-JAC.2 (2012) 11-17.

[14] A. Kesraoui Abdessalem, N. Bellakhal, N. Oturan ,M. Dachraoui, M. A. Oturan, "Treatment of a mixture of three pesticides by photo- and electro-Fenton processes", Desalination 250 (2010) 450–455.

[15] M. Antonopoulou, I. Konstantinou, "Photocatalytic treatment of metribuzin herbicide over TiO_2 aqueous suspensions: Removal efficiency, identification of transformation products, reaction pathways and ecotoxicity evaluation", Journal of Photochemistry and Photobiology A: Chemistry 294 (2014) 110–120.

[16] M. Houari, M. Saidi, D. Tabet, P. Pichat, H. Khalaf, "The removal of 4-chlorophenol and dichloroacetic acid in water using Ti-, Zr- and Ti/Zr-pilarred bentonites as photocatalyst", Am. J. Applied. Sci. 2 (2005) 1136–1140.

[17] O.Carp, C.L.Huisman, A.Reller, "Photoinduced reactivity of titanium dioxide", Prog. Solid State Chem. 32, (2004) 33–177.

[18] J.-M.Herrmann, "Heterogeneous photocatalysis: fundamentals and applications to the removal of various types of aqueous pollutants", Catal. Today 53 (1999) 115–129.

[19] J. Liu, M. Dong, S. Zuo, Y. Yu, "Solvothermal preparation of TiO_2/montmorillonite and photocatalytic activity", Applied Clay Science 43 (2009) 156–159.

[20] Z. Sun, Y. Chen, Q. Ke, Y. Yang, J. Yuan, "Photocatalytic degradation of a cationic azo dye by TiO_2/bentonite nanocomposite", J. Photochem. Photobiol. A: Chem. 149 (2002) 169–174.

[21] M. Mahalakshmi, S. Vishnu Priya, B. Arabindoo, M. Palanichamy, V. Murugesan, "Photocatalytic degradation of aqueous propoxur solution using TiO_2 and Hb zeolite-supported TiO_2", J. Haz. Mater. 161 (2009) 336–343.

[22] M.N. Chong, V. Vimonses, S. Lei, B. Jin, C. Chow, C. Saint, "Synthesis and characterization of novel titania impregnated kaolinite nano-photocatalyst", Micropor. Mesopor. Mater. 117 (2009) 233–242.

[23] Z.M. Xie Chen, Y.Z. Dai, "Preparation of TiO_2/sepiolite photocatalyst and its application to printing and dyeing wastewater treatment", Environ. Sci. Technol. 32 (2009) 123–127.

[24] Y. Kameshima, Y. Tamura, A. Nakajima, K. Okada, "Preparation and properties of TiO_2/montmorillonite composites", App. Clay Sci. 45 (2009) 20–23.

[25] R. Trujillano , M. A. Vicente, V. Rives, S. A. Korili, A. Gil, K. J. Ciuffi, E. J. Nassar, "Preparation, alumina-pillaring and oxidation catalytic performances of synthetic Ni-saponite", Desalination 250 (2010) 450–455.

[26] A. Darehkordi1, S. M. Sadegh Hosseini1, and M. Tahmooresi, "Montmorillonite modified as an efficient and environment friendly catalyst for one-pot synthesis of 3, 4-Dihydropyrimidine-2 (1H) ones", Iranian Journal of Materials Science & Engineering Vol. 9, Number 3 (2012).

[27] L. –A. Galeano, M. Á. Vicente, A. Gil, "Catalytic Degradation of Organic Pollutants in Aqueous Streams by Mixed Al/M-Pillared Clays (M = Fe, Cu, Mn)", Catalysis Reviews: Science and Engineering, 56:3 (2014) 239-287.

[28] J. P.Sterte, "Clays Clay Minerals", 34 (1986), 658.

[29] S. Yamanaka, T. Nisihara, M. Hattori, "Preparation and properties of titania pillared clay", Mater. Chem. Phys. 17, (1987) 87–101.

[30] I. Fatimah, S. Wang, K. Wijaya, "Composites of TiO_2-aluminum pillared montmorillonite: synthesis, characterization and photocatalytic degradation of methylene blue", App. Clay Sci. 50 (2010) 588–593.

[31] L. Sciascia, M. Liri Turco Liveri, M. Merli, "Kinetic and equilibrium studies for the adsorption of acid nucleic bases onto K10 montmorillonite", Applied Clay Science 53 (2011) 657–668.

[32] P.Komadel, J.Madejova, "Acid activation of clay minerals". In: Bergaya, F., Theng, B.K.G., Lagaly, G. (Eds.), Handbook of Clay Science. Elsevier (2006) 263–288.

[33] J. Arfaoui, L. Khalfallah Boudali, A. Ghorbel, "Vanadia-doped titanium-pillared clay: Preparation, characterization and reactivity in the epoxidation of allylic alcohol (E)-2-hexen-1-ol", Catalysis Communications 7 (2006) 86–90.

[34] J.P. Jolivet, « De la solution à l'oxyde: Condensation des cations en solution aqueuse, chimie de surface des oxydes », International. editions/CNRS edition Paris (1994), 387.

[35] C. Blanco, , F. Gonzalez, , C. Pesquera, , I. Benito, , S. Mendioroz, J.A. Pakhares, "Differences between one palygorskite and another magnesic by infrared spectroscopy", Spectrosc. Lett. 22 (6) (1989) 659–673.

[36] S. Caillère, S. Hénin, M. Rautureau, « Minéralogie des argiles », Tomes 1 et 2. Paris: Masson (1982) 189.

[37] V. C. Farmer, "The Infrared Spectra of Minerals", Mineralogical Society, Monograph 4, London, (1974) 539.

[38] P. Salerno, M. B. Asenjo, S. Mendiorez, "Influence of preparation method on thermal stability and acidity of Al–PILCs", Thermochimica Acta, 379 (2001) 101-109.

[39] M. Burgos and M. Langlet, "The Sol-Gel Transformation of TIPT Coatings: A FTIR Study",Thin Solid Films, Vol. 349, No. 1-2 (1999) 19-23.

[40] F. N. Castellano, J. M. Stipkala, L. A. Friedman and G. L. Meyer, "Spectroscopic and Excited-State Properties of Titanium-Dioxide Gels", Chemistry of Materials, Vol. 6, No. 11 (1994) 2123-2129.

[41] M. Kurian, S.Sugunan, "Liquid phase benzylation of o-xylene over pillared clays", Ind. J. Chem. 42 A (2003) 2480–2486.

[42] C. Ooka, H. Yoshida, K. Suzuki, T. Hattori, Microporous Mesoporous Mater. 67 (2004) 143–150.

[43] S.W. Karickhoff, G.W. Bailey, Clay. Clay Miner. 21 (1973) 59–70.

[44] Y.Segura, L.Chmielarz, P.Kustrowski, P.Cool, R.Dziembaj, E.F.Vansant, Appl. Catal. B 61 (2005) 69.

[45] H. Chamley. Clay Sedimentology. Springer, Berlin (1989), 623.

[46] W.D. Keller, "The nascence of clay minerals", Clays and Clay Minerals (1985), 33, 161-172.
[47] M.D. Wilson and E.D. Pittman, "Authigenic clays in sandstones: Recognition and influence of reservoir properties and paleoenvironmental analysis", Journal of Sedimentary Petrology (1977), 47, 331.
[48] M. Tahir, B. Tahir, N. Saidina Amin, "Photocatalytic CO_2 reduction by CH_4 over montmorillonite modified TiO_2 nanocomposites in a continuous monolith photoreactor", Materials Research Bulletin 63 (2015) 13–23.
[49] S.J.Gregg, K.S.W.Sing, "Adsorption surface area and porosity", Academic Press, London(1982).
[50] L. Chmielarz, Z. Piwowarska, P. Kuśtrowski, A. Węgrzyn, B. Gil, A. Kowalczyk, B. Dudek, R. Dziembaj, M. Michalik, "Comparison study of titania pillared interlayered clays and porous clay heterostructures modified with copper and iron as catalysts of the DeNOx process", Applied Clay Science 53 (2011) 164–173.
[51] J.-T. Lin, S.-J. Jong, S. Cheng, "A new method for preparing microporous titanium pillared clays", Microporous Materials, 1 (1993) 281-290.
[52] H. Mao, K. Zhu, B. Lia, C. Yao, Y. Kong, "Synthesis of titania modified silica-pillared clay (SPC) with highlyordered interlayered mesoporous structure for removing toxic metalion Cr(VI) from aqueous state", Applied Surface Science (2014).
[53] C.F. Baes Jr., R.E. Mesmer, "Hydrolysis of Cations", Wiley, New York (1976).
[54] J.D. Ellis, G.A.K. Thompson, Inorg. Chem. 15 (1976) 3172.
[55] Y. Zhang, D. Wang, G. Zhang, "Photocatalytic degradation of organic contaminants by TiO_2/sepiolite composites prepared at low temperature", Chemical Engineering Journal 173 (2011) 1– 10.
[56] I.K.Konstantinou, T.A. Albanis, "TiO_2-assisted photocatalytic degradation of azo dyes in aqueous solution: kinetic and mechanistic investigations—A review", Appl. Catal. B: Environ. 49 (2004) 1–14.
[57] M. Saquiba, M.A. Tariqa, M. Faisala, M. Muneer, "Photocatalytic degradation of two selected dye derivatives in aqueous suspensions of titanium dioxide", Desalination 219 (2008) 301–311.
[58] L.-C. Chen, C.-M. Huang, F.-R. Tsai, "Characterization and photocatalytic activity of K+-doped TiO_2 photo catalysts", J. Mol. Catal. A: Chem. 265 (2007) 133–140.
[59] M. Huang, C. Xu, Z. Wu, Y. Huang, J. Lin, J. Wu, "Photocatalytic discolorization of methyl orange solution by Pt modified TiO_2 loaded on natural zeolite", Dyes Pigm. 77 (2008) 327–334.
[60] S. Chakrabarti, B.K. Dutta, "Photocatalytic degradation of model textile dyes in wastewater using ZnO as semiconductor catalyst", J. Hazard. Mater. B 112 (2004) 269–278.
[61] J. Sun, L. Qiao, S. Sun, G. Wang, "Photocatalytic degradation of Orange G on nitrogen-doped TiO_2 catalysts under visible light and sunlight irradiation", J. Hazard. Mater. 155 (2008) 312–319.
[62] U.G. Akpan, B.H. Hameed, "Parameters affecting the photocatalytic degradation of dyes using TiO_2-based photocatalysts: A review", Journal of Hazardous Materials 170 (2009) 520–529.
[63] H. Lachheb, E. Puzenat, A. Houas, M. Ksibi, E. Elaoui, G. Guillard, J.M. Hermann, "Photocatalytic degradation of various types of dyes (alizarin S, crecein OrangeG, methyl red, congo red, methylene blue) in water by UV-irradiated titania", Appl. Catal. B: Environ. 39 (2002) 75–90.
[64] M. Stylidi, D.I. Kondarides, X.E. Verykios, "Pathways of solar light-induced photocatalytic degradation of azo dyes in aqueous TiO_2 suspension", Appl. Catal. B: Environ. 40 (2003) 271–286.